tvst

Article

Establishment and Comparison of Algorithms for Detection of Primary Angle Closure Suspect Based on Static and Dynamic Anterior Segment Parameters

Ye Zhang[1], Qing Zhang[2], Lei Li[1], Ravi Thomas[3,4], Si Zhen Li[5], Ming Guang He[6,7,8], and Ning Li Wang[1,2]

[1] Beijing Tongren Eye Center, Beijing Key Laboratory of Ophthalmology and Visual Science, Beijing Tongren Hospital, Capital Medical University, Beijing, China
[2] Beijing Institute of Ophthalmology, Beijing, China
[3] Queensland Eye Institute, Brisbane, Australia
[4] University of Queensland, Brisbane, Australia
[5] Nanjing Tongren Hospital, Jiangsu, China
[6] State Key Laboratory of Ophthalmology, Zhongshan Ophthalmic Center, Sun Yat-sen University, Guangzhou, China
[7] Department of Surgery, University of Melbourne, Melbourne, Australia
[8] Ophthalmology, Centre for Eye Research Australia, Melbourne, Australia

Correspondence: Ning Li Wang, Beijing Institute of Ophthalmology, Beijing Tongren Eye Center, Beijing Tongren Hospital, Capital Medical University; Beijing Key Laboratory of Ophthalmology and Visual Sciences. No. 1 Dong Jiao Min Xiang Street, Dongcheng District, Beijing 100730, People's Republic of China. e-mail: wningli@vip.163.com

Received: October 2, 2019
Accepted: February 12, 2020
Published: April 23, 2020

Keywords: primary angle closure suspect; screening; iris dynamic changes; machine-learning algorithms

Citation: Zhang Y, Zhang Q, Li L, Thomas R, Li SZ, He MG, Wang NL. Establishment and comparison of algorithms for detection of primary angle closure suspect based on static and dynamic anterior segment parameters. Trans Vis Sci Tech. 2020;9(5):16, https://doi.org/10.1167/tvst.9.5.16

Purpose: To establish and evaluate algorithms for detection of primary angle closure suspects (PACS), the risk factor for primary angle closure disease by combining multiple static and dynamic anterior segment optical coherence tomography (ASOCT) parameters.

Methods: Observational, cross-sectional study. The right eyes of subjects aged ≥40 years who participated in the 5-year follow-up of the Handan Eye Study, and underwent gonioscopy and ASOCT examinations under light and dark conditions were included. All ASOCT images were analyzed by Zhongshan Angle Assessment Program. Backward logistic regression (BLR) was used for inclusion of variables in the prediction models. BLR, naïve Bayes' classification (NBC), and neural network (NN) were evaluated and compared using the area under the receiver operating characteristic curve (AUC).

Results: Data from 744 subjects (405 eyes with PACS and 339 normal eyes) were analyzed. Angle recess area at 750 µm, anterior chamber volume, lens vault in light and iris cross-sectional area change/pupil diameter change were included in the prediction models. The AUCs of BLR, NBC, and NN were 0.827 (95% confidence interval [CI], 0.798-0.856), 0.826 (95% CI, 0.797-0.854), and 0.844 (95% CI, 0.817-0.871), respectively. No significant statistical differences were found between the three algorithms ($P = 0.622$).

Conclusions: The three algorithms did not meet the requirements for population-based screening of PACS. One possible reason could be the different angle closure mechanisms in enrolled eyes.

Translational Relevance: This study provides a promise for basis for future research directed toward the development of an image-based, noncontact method to screen for angle closure.

Introduction

Primary angle closure glaucoma (PACG), a leading cause of ocular morbidity will affect approximately 21 million people worldwide by 2020; China has the largest number of cases (about 48% of the total).[1] If left untreated, PACG can lead to severe irreversible visual impairment.[2] In China, approximately 5.2 million people are blind in one eye and 1.7 million of these are blind in both eyes from PACG.[2]

Primary angle closure suspect (PACS) is a risk factor for primary angle closure disease (PACD). PACD includes primary angle closure (PAC, defined as PACS with raised intraocular pressure [IOP] and / or peripheral anterior synechia [PAS]) and PACG (PAC with the presence of typical glaucomatous optic neuropathy or visual field defects).[3] Thomas et al reported that, over 5 years, 22% of PACS progressed to PAC and 28% of the latter progressed to PACG.[4–5]

Iridotomy performed for PACS can decrease progression to PAC and PACG.[6–8] Hence, early screening and detection of PACD, especially at the PACS and early PAC stages would be valuable for control of the disease and prevention of visual impairment caused by PACG.[9]

The current gold standard for angle-closure assessment is gonioscopy; this is a contact-based, subjective, and examiner-dependent technique with moderate reproducibility.[10,11] Accordingly, gonioscopy is not an optimal tool for large-scale population-based screening.[11] A test for population-based screening should be noncontact, easy to perform, clinician independent, reproducible with a high specificity and moderate sensitivity.[12]

Several noncontact imaging devices of the angle are available including Scheimpflug imaging (Pentacam) and anterior chamber segment optical coherence tomography (ASOCT).[10] However, none of them are considered as an ideal screening test for PACD.[13] Possible reasons for the poor performance of these tests in screening may be failing to include essential risk factors of PACD and using only one risk factor as the screening parameter in early detection of PACD.

Various factors, including age, shorter axial length (AXL), increased iris thickness, and shallow anterior chamber, a thick, anteriorly positioned lens and a large lens vault (LV) have been reported to be associated with PACD.[14,15] A low central anterior chamber depth (ACD) is a risk factor for angle closure that is easily evaluated and commonly used as a screening tool.[13] Recent studies suggest that the pathogenesis of PACD depends not only on static anatomical factors but also on different dynamic responses of the iris under light and dark conditions as well as changes in the choroid.[16–19] To the best of our knowledge, dynamic risk factors have not been evaluated for the screening of PACD.

We undertook this study to establish and compare predictive models created from different machine-learning techniques based on the concept of combining multiple static and dynamic ASOCT parameters as a screening tool to detect PACS.

Methods

Subjects and Ophthalmic Examination

This observational, cross-sectional study was part of the 5-year follow-up of the Handan Eye Study(HES) conducted on a sample of rural Chinese adults aged 35 years or older living in the Handan County, Hebei Province.[20] HES subjects aged $\geq$ 40 years who participated in this follow-up examination between June 2012 and May 2013, with limbal anterior chamber depth $\leq$ 40% and underwent gonioscopy and ASOCT examinations under light and dark conditions were eligible.

Eyes with PAS, raised IOP, cup-disc ratio $\geq$ 0.6 or presence of typical glaucomatous optic neuropathy, secondary angle closure, past history of an acute angle closure attack, laser peripheral iridotomy (LPI) or iridoplasty, ocular surface pathology, eye trauma, intraocular surgery, and use of eyedrops that could influence anterior chamber angle were excluded. Other exclusion criteria were inability to fixate on the target and general physical or mental impairment that precluded testing. The right eye of each subject was included for analysis.

The study was conducted in accordance with the tenets of the Declaration of Helsinki and approved by the Ethics committee at Beijing Tongren Hospital. Written informed consent was obtained from all subjects.

All subjects underwent detailed and standardized ocular examinations, including presenting visual acuity (PVA) and best-corrected visual acuity using the Early Treatment Diabetic Retinopathy Study LogMAR E chart, objective refraction using a KR-8800 auto kerato-refractometer (Topcon, Tokyo, Japan) and subjective refraction, slit-lamp examination, IOP measurement using a Kowa applanation tonometer, A-scan ultrasound biometry using an OcuScan RxP (Alcon, Inc., Fort Worth, TX), and stereoscopic optic disc examination with a 90-diopter lens. Static gonioscopy was performed in a dark room by one of the two glaucoma specialists using a Goldmann type one-mirror lens with the eye in the

primary gaze position. Dynamic examination (indentation gonioscopy) with increased illumination was performed after static gonioscopy, using the same lens to assess angle opening and evaluate for PAS. The specialists performing gonioscopy were masked to ASOCT findings. PACS was diagnosed if ≥ 180° of the posterior trabecular meshwork was not visible on static gonioscopy.

ASOCT Image Acquisition and Analysis

Anterior segment optical coherence tomography (Visante; Carl Zeiss Meditec, Inc., Dublin, CA) uses a long wavelength (1310 nm) to optimize visualization of the iridocorneal angle and a cross section of anterior segments in the absence of visible light influence on angle configuration and pupil size.[10,21] Each eye was imaged with an ASOCT first under dark conditions (~3 lux, to induce physiologic mydriasis) and then with light (~200 lux). The subjects adapted to the dark for at least 3 minutes before examination. During ASOCT scanning, an internal fixation target was used with the subjects' refractive correction in place to perform the measurements in an unaccommodated state. All the ASOCT scans were performed by a trained ophthalmic technician masked to the subjects' examination data.

All images were obtained in the "anterior segment quadrant" mode at the 0° to 180°, 45° to 225°, 90° to 270°, and 135° to 315° meridians. Imaging was repeated if the scleral spur visibility was poor; the best set of images were selected. The Zhongshan Angle Assessment Program (Guangzhou, China) was used to analyze the ASOCT images.[22]

Once the location of two scleral spurs on each image was determined by one ophthalmologist (Z.Y.), the following angle and anterior chamber configuration parameters were measured: angle opening distance at 500 μm (AOD500), trabecular-iris space area at 500 μm (TISA500), angle recess area at 750 μm (ARA750), anterior chamber area (ACA), anterior chamber volume (ACV), anterior chamber width (ACW), iris thickness at 750 μm (IT750), iris curvature (IC), iris cross-sectional area (IA), LV, and pupil diameter (PD).[22]

AOD500 is the perpendicular distance from the point at 500 μm from the scleral spur to the anterior iris surface and TISA500 is the area bounded by the AOD500, the anterior iris surface, the inner corneoscleral wall, and the perpendicular distance between the scleral spur and the opposing iris.[23] ARA750 is the area bordered by the anterior iris surface, corneal endothelium, and a line perpendicular to the corneal endothelium drawn to the iris surface from a point at 750 μm anterior to the scleral spur.[23] The ACA is defined as the cross-sectional area of the anterior segment bounded by the corneal endothelium, anterior surface of the iris, and anterior surface of the lens. The ACV is derived by rotating anterior chamber area 360° around a vertical axis.[24] The ACW was measured as the horizontal scleral spur-to-spur distance.[25]

The IT750 is defined as the iris thickness measured at 750 μm from the scleral spur and the IC is determined by measuring the maximum distance between the posterior iris surface and a line from the iris root to the first point of contact between the iris and lens.[25] The LV was defined as the perpendicular distance between the anterior pole of the lens and the horizontal line joining the scleral spurs.[26] The PD is automatically measured as the distance between the pupillary tips of the iris on both sides on the cross-sectional images.[25] The IA is defined as the cross-sectional area of the nasal and temporal sides.[27] IA change was calculated as IA in light minus IA in dark. PD change was calculated as PD in dark minus PD in light. IA change/PD change was calculated as the IA change divided by the PD change. Eyes with a PD increase of less than 0.5 mm after physiologic mydriasis were excluded.

Statistical Analysis

Three prediction algorithms for the detection of PACS were evaluated: backward logistic regression (BLR), naïve Bayes' classification (NBC), and neural network (NN).[28] The three methods are summarized as follows:

1. Logistic regression is a well-established classification technique that is widely used in epidemiological studies.[28] In backward logistic regression, the least significant effect that does not meet the level for staying in the model is removed. Once an effect is removed from the model, it remains excluded. The process is repeated until no other effect in the model meets the specified level for removal.[29]
2. Naïve Bayes' classification estimates the probability that an observation is in a particular class based on its covariate values under the assumption that the covariates are independent conditional on class membership and, if they are continuous, are normally distributed.[28] The algorithm works well with heterogeneous data types and also with missing values, because of the independent treatment of each predictor variable for model construction.[30]
3. NN comprises layers of interconnected artificial neurons.[31] An artificial neuron is designed based on the biological neuron itself and receives multiple inputs multiplied by weights; it outputs the sum of the inputs.[31] It is equivalent to logistic regression

but can solve more difficult problems with more complex network architectures.[28,30] The price of using complex architectures is that it produces models that are more difficult to interpret.[30]

BLR was used for inclusion of variables in the prediction models. There were 12 parameters under two conditions respectively: AOD500, TISA500, ARA750, IT750, IC, LV, ACD, ACW, ACA, ACV, IA, and PD. And plus two calculated parameters of changes from dark to light conditions including IA change and IA change/PD change, there were a total of 26 candidate parameters for inclusion of variables in the prediction models. First of all, we used the univariate logistic regression analysis (backward) on the 26 parameters and excluded the variables with a *P* value more than 0.05.

Then, to avoid the obvious correlations between the independent variables, we designed four combinations of variables for multivariate logistic regression analysis (backward) to build the models: (1) 12 parameters under light conditions plus IA change; (2) 12 parameters under light conditions plus IA change/PD change; (3) 12 parameters under dark conditions plus IA change; and (4) 12 parameters under dark conditions plus IA change/PD change. The variance inflation factors and clinical significance of included factors were calculated and considered to determine the included variables in multivariate logistic regression analysis of each model. Significant variables with a *P* value < 0.1 in the multivariate analysis were used to produce each logistic model. The Nagelkerke R squares were calculated to evaluate the four logistic models and to select the best logistic model that fitted the data. The variables selected through BLR analysis were also used to build the NBC and the NN models.

The three prediction models created were evaluated and compared in terms of point and interval estimates of the area under the receiver operating characteristic curve (AUC), sensitivity and specificity. The receiver operating characteristic (ROC) plot expresses the relationship between sensitivity and 1–specificity. The closer the ROC curve is located to upper-left hand corner, the better the model.[32] The AUC can have any value between 0 and 1 and it is a good indicator of the goodness of the model.[32] The sensitivity of a model refers to the ability of the model to correctly identify those patients with the disease and the specificity refers to the ability of the test to correctly identify those patients without the disease.[32]

Statistical analysis was performed using the Statistical Analysis System (SAS), version 9.4 (SAS Institute, Cary, NC). P values < 0.05 were considered statistically significant. The estimates of AUC (95% confidence interval [CI]), sensitivity, and specificity of three models were analyzed using the Statistical Package for Social Sciences (SPSS), version 25 (SPSS, Chicago, IL).

Results

A total of 989 subjects who completed the ocular examinations as well as gonioscopy and ASOCT measurements under light and dark conditions were included. A total of 202 eyes were excluded for the following reasons: 132 eyes (13.3%) had poor-quality ASOCT images or scleral spurs that could not be accurately determined; 70 eyes had PD change less than

Table 1. Demographic Data and Ocular Biometric Measurements in PACS and Normal Subjects

Parameter	Normal Subjects (n = 339)	PACS Subjects (n = 405)	*P* Value
Age (IR), years	61.0 (56.0, 66.0)	62.0 (57.0, 67.0)	0.119†
Male (%)	121 (35.7)	125 (30.9)	0.163‡
Female (%)	218 (64.3)	280 (69.1)	
PVA (IR)	0.20 (0.10–0.32)	0.30 (0.12–0.44)	<.001†
BCVA (IR)	0.00 (0.00–0.18)	0.08 (0.00–0.20)	0.025†
SE (IR), diopter	0.50 (-0.25–1.13)	0.81 (0.25–1.50)	<0.001†
IOP (IR), mm Hg	12.0 (10.0–13.5)	11.5 (10.0–13.0)	0.086†
CCT (IR), mm	528 (510–545)	528 (514–548)	0.282†
Central ACD (IR), mm	2.71 (2.49–2.92)	2.51 (2.33–2.76)	<0.001†
LT (IR), mm	4.79 (4.51–5.07)	4.86 (4.53–5.11)	0.139†
AL (IR), mm	22.73 (22.19–23.27)	22.28 (21.81–22.97)	0.001†

ACD, anterior chamber depth; AL, axial length; BCVA, best corrected visual acuity; CCT, central corneal thickness; IOP, intraocular pressure; IR, interquartile range; LT, lens thickness; PVA, presenting visual acuity; SE, spherical equivalent.

†Mann-Whitney *U* test.

‡χ^2 test.

Table 2. Anterior Chamber, Angle, Lens, and Iris Parameters Measured by ASOCT in Light and Dark Conditions in PACS and Normal Subjects

Conditions	Parameter	Normal Subjects (n = 339)	PACS Subjects (n = 405)	*P* Value*
Light	AOD500 (IR), mm	0.349 (0.286–0.448)	0.249 (0.183–0.313)	<0.001†
	TISA500 (IR), mm^2	0.144 (0.120–0.181)	0.103 (0.076–0.131)	<0.001†
	ARA (IR), mm^2	0.406 (0.322–0.488)	0.269 (0.193–0.345)	<0.001†
	ACD (IR), mm	2.488 (2.321–2.639)	0.245 (2.072–2.401)	<0.001†
	ACW (SD), mm	11.10 (0.40)	10.87 (0.42)	<0.001‡
	ACA (IR), mm^2	18.26 (16.60–19.81)	15.85 (14.25–17.25)	<0.001†
	ACV (IR), mm^3	73.61 (65.26–82.33)	60.40 (53.41–68.18)	<0.001†
	IT750 (IR), mm	0.44 (0.39–0.48)	0.47 (0.43–0.50)	<0.001†
	IC (SD), mm	0.24 (0.19–0.28)	0.26 (0.21–0.31)	<0.001‡
	LV (IR), mm	252.3 (111.1–393.3)	415.9 (287.2–516.5)	<0.001†
Dark	AOD500 (IR), mm	0.309 (0.252–0.388)	0.211 (0.138–0.278)	<0.001†
	TISA500 (IR), mm^2	0.129 (0.105–0.156)	0.084 (0.059–0.111)	<0.001†
	ARA (IR), mm^2	0.329 (0.266–0.408)	0.206 (0.142–0.278)	<0.001†
	ACD (IR), mm	2.483 (2.327–2.633)	2.251 (2.066–2.402)	<0.001†
	ACW (IR), mm	11.08 (10.80–11.33)	10.94 (10.69–11.19)	<0.001†
	ACA (IR), mm^2	18.60 (16.96–20.25)	16.24 (14.63–17.79)	<0.001†
	ACV (IR), mm^3	74.47 (66.57–83.86)	62.76 (54.23–70.95)	<0.001†
	IT750 (IR), mm	0.47 (0.42–0.51)	0.49 (0.46–0.53)	<0.001†
	IC (IR), mm	0.24 (0.20–0.28)	0.25 (0.21–0.30)	<0.001†
	LV (IR), mm	276.4 (136.3–390.3)	418.9 (303.5–558.1)	<0.001†

ACA, anterior chamber area; ACD, anterior chamber depth; ACV, anterior chamber volume; ACW, anterior chamber width; AOD500, angle opening distance at 500 µm; ARA750, angle recess area at 750 µm; IC, iris curvature; IT750, iris thickness at 750 µm; IR, interquartile range; LV, lens vault; SD, standard deviation; TISA500, trabecular-iris space at 500 µm.

†Mann-Whitney *U* test.

‡Two sample *t*-test.

0.5 mm from dark to light conditions. Data from the right eye of 744 remaining subjects were included in the final analysis; 498 (66.9%) were female. The mean age was 61.39 ± 8.27 years. There were no statistically significant differences in demographic or ocular features between those included and excluded.

The demographic characteristics and ocular biometric data of subjects are summarized in Table 1. There were 405 PACS (54.4%) and 339 normal subjects. Compared with normal subjects those with PACS had worse PVA ($P < 0.001$), worse best-corrected visual acuity ($P = 0.025$), larger spherical equivalence ($P < 0.001$), smaller ACD ($P < 0.001$), and shorter AXL ($P < 0.001$). There was no significant difference in age, sex, IOP, central corneal thickness, and lens thickness (LT) between the two groups.

The mean values and the absolute and relative changes when going from dark to light for ASOCT parameters in PACS and normal subjects and the differences between the groups are summarized in Tables 2 and 3. Compared with normal subjects, PACS had smaller AOD500 ($P < 0.001$), TISA500 ($P < 0.001$), ARA ($P < 0.001$), ACD ($P < 0.001$), ACW ($P < 0.001$), ACA ($P < 0.001$), ACV ($P < 0.001$), IT750 ($P < 0.001$), IC ($P < 0.001$), LV ($P < 0.001$) in light and dark conditions, and smaller IA change ($P < 0.001$), PD change ($P = 0.001$), and IA change/PD change ($P = 0.001$) from dark to light conditions. All differences were statistically significant.

The logistic model with a combination of parameters measured under light conditions plus IA change/PD change as included variables was determined to be the best one (Nagelkerke $R^2 = 0.413$). The following four variables were included in the prediction models using BLR (Table 4): ARA750 in light ($P < 0.001$), ACV in light ($P = 0.003$), LV in light ($P = 0.005$), and IA change/PD change ($P = 0.004$). Table 5 shows the prediction accuracies of the three algorithms.

Table 3. ASOCT Data: IA, PD, IA Changes and IA Changes per PD Changes for PACS and Normal Subjects

Parameter	Normal Subjects (n = 339)	PACS Subjects (n = 405)	*P* Value*
IA; L (SD), mm^2	2.94 (0.37)	2.90 (0.39)	0.155‡
PD; L (SD), mm	3.82 (0.64)	3.90 (0.64)	0.113‡
IA; D (SD), mm^2	2.69 (0.34)	2.71 (0.37)	0.383‡
PD; D (IR), mm	4.86 (4.25–5.28)	4.81 (4.34–5.23)	0.952†
IA Change; D (IR), mm^2	0.25 (0.13–0.39)	0.20 (0.03–0.35)	<0.001†
PD Change; D (IR), mm	0.88 (0.61–1.18)	0.74 (0.31–0.35)	0.001†
IA Change / PD Change (IR), mm	0.26 (0.16–0.36)	0.22 (0.05–0.37)	0.001†

D, dark; IA, iris cross-sectional area; IR, interquartile range; L, light; PD, pupil diameter; SD, standard deviation.
†Mann-Whitney *U* test.
‡Two sample *t*-test.

Table 4. Variables Included in the Prediction Models Using Backward Logistic Regression

Parameter	Estimated Regression Coefficient	Standard Error	χ^2	*P* Value	OR (95% CI)
ARA750	-7.846	1.112	49.764	<0.001	<0.001 (<0.001–0.003)
ACV	-0.029	0.010	8.863	0.003	0.971 (0.953–0.990)
LV	0.001	0.001	7.741	0.005	1.001 (1.000–1.003)
IA change/PD change	-1.014	0.353	8.272	0.004	0.363 (0.182–0.724)

ACV, anterior chamber volume; ARA750, angle recess area at 750 µm; CI, confidence interval; IA, iris cross-sectional area; LV, lens vault; OR, odds ratio; PD, pupil diameter.

Table 5. AUC, Sensitivity, and Specificity of Algorithms

Prediction Algorithm	AUC	95% CI of of AUC	Sensitivity	95% CI of Sensitivity	Specificity	95% CI of Specificity
Backward logistic Regression	0.827	0.798–0.856	72.35%	67.99–76.71	78.17%	73.77–82.57
Naïve Bayes' classification	0.826	0.797–0.854	72.84%	68.51–77.17	76.40%	71.88–80.92
Neural network	0.844	0.817–0.871	78.02%	73.98–82.05	74.93%	70.32–79.54

AUC, area under the receiver operator characteristic curve; CI, confidence interval.

The Figure shows the ROC curves of the 3 algorithms. The AUCs and 95% CIs of BLR, NBC, and NN were 0.827, (95% CI, 0.798–0.856), 0.826 (95% CI, 0.797–0.854), and 0.844 (95% CI, 0.817–0.871) respectively. There were no statistically significant differences between the three algorithms ($P = 0.622$).

BLR had a sensitivity of 72.35% (95% CI, 67.99%–76.71%) and a specificity of 78.17% (95% CI, 73.77%–82.57%). NBC showed a sensitivity of 72.84% (95% CI, 68.51%–77.17%) and a specificity of 76.40% (95% CI, 71.88%–80.92%). NN provided a sensitivity of 78.02% (95% CI, 73.98%–82.05%) and a specificity of 74.93% (95% CI, 70.32%–79.54%).

Discussion

The two main approaches for the systematic detection of early PACD are population-based screening and case detection (also known as opportunistic screening).[12] To date, there is no ideal population-based screening test for PACD, which requires a high specificity with moderate sensitivity.[12]

We hypothesized that the possible reasons for the lack of an ideal early screening test for PACD were failure to include risk factors other than ACD as screening parameters and not using a combination of

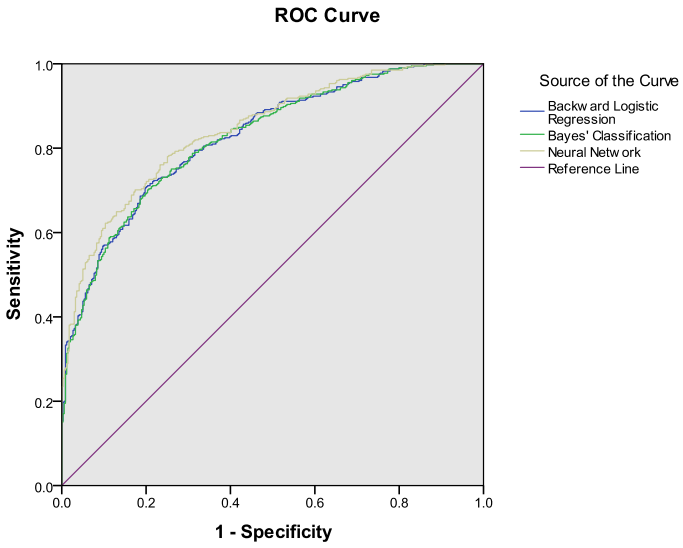

Figure Receiver operating characteristic curves of three machine-learning algorithms

risk factors for PACD. Accordingly, we tried to build a predictive model for early screening of PACD using classification algorithms based on static and dynamic ASOCT measurements.

Use of machine-learning techniques is still new in this field.[32] They have been used in detection and diagnosis of glaucoma.[32,33] To the best of our knowledge, no studies that use machine-learning algorithms or combine the static and dynamic ASOCT parameters in the early screening of PACD have been published.

In our study, three machine-learning algorithms including BLR, NBC, and NN for the detection of PACS were created and compared. These algorithms were found to have good AUCs but still failed to meet the need of a high specificity and moderate sensitivity required for population-based screening of PACD.

Nongpiur et al reported that a classification algorithm based on stepwise logistic regression that used a combination of six parameters obtained from a single horizontal ASOCT scan identified subjects with gonioscopic angle closure 95% of the time, with an AUC of 0.954 (95% CI, 0.942-0.966).[34] Differences in predictive power across that study and ours can be ascribed to different characteristics of the datasets, different stages of the disease, different angle closure mechanisms involved and different candidate variables for building and evaluating the models.

Diagnostic test accuracy may vary according to the severity of the disease.[35] According to our previous study and other publications, eyes with different stages of PACD have statistically significant differences in ASOCT parameters.[18,36–37]

Guzman et al. reported that compared with PAC and PACG, the PACS eyes had wider anterior chamber angles as well as a more spacious anterior chamber characterized by larger ACA, ACV, deeper ACD, and a smaller LV.[36] Lin et al reported that PACG eyes had smaller ACD and ACA in both light and dark conditions, smaller AOD500, ARA750, and IA in light, and smaller IT in dark than PACS/PAC eyes.[37] They also found that PACG eyes had smaller IA change from light to dark conditions compared with PACS/PAC eyes.[37]

We have reported that PAC/PACG eyes had smaller AOD500, TISA500, and ARA and larger LV than PACS eyes.[18] It seems that eyes with different stages of PACD have different ASOCT parameters. Hence, the accuracy of these models is likely to vary with the stage of PACD. Moreover, the accuracy may also vary among PACS with different angle closure mechanisms.

In a previous study, we categorized enrolled PACD eyes into three subgroups: pupillary block (PB), plateau iris configuration (PIC) and thick peripheral iris roll (TPIR), according to their dominant angle closure mechanisms as determined by ASOCT images.[17] We demonstrated that PACD eyes with PB had the smallest ACD, ACW, ACA, ACV, AXL, and largest LT, whereas PACD eyes with PIC had the largest ACD, ACW, ACA, ACV, AXL, and smallest LT.[17] PACD eyes with TPIR had the smallest AOD500, TISA500, and ARA750.[17]

Baek et al reported two different clusters based on ASOCT images from the total angle closure population.[38] One cluster was characterized by relatively higher ACD and ACA, lower LV, thicker peripheral iris, and higher ACW which could be attributed to plateau iris configuration or thick peripheral iris.[38] The second cluster was characterized by higher LV, smaller AXL, smaller ACW, and lower ACA, which may be attributed to the lens or crowding of intraocular structures in eyes with smaller dimensions.[38]

Nongpiur et al identified three subgroups among PACS eyes based on ASOCT images.[39] Subgroup 1 was characterized by a greater IA and IT. Subgroup 2 was characterized by a smaller ACD, ACA, ACW, AXL, and greater LV. Subgroup 3 was characterized by elements of both subgroups 1 and 2.[39]

Moghimi et al also reported three different angle closure subtypes among PACS, PACG, acute primary angle closure, and the fellow eyes of acute primary angle closure using statistical clustering analysis based on ASOCT parameters.[40] Cluster 1 had the smallest ACD and ACA, as well as the largest LV, suggesting a pushing mechanism as a result of the forward movement of the lens and increased LT.[40] Cluster 2 had the largest IT at 2000 μ, largest IA, and deepest

ACD, which may result in angle crowding and subsequent angle closure due to a predominant iris component.[40] Cluster 3 was characterized by elements of both clusters 1 and 2 and a higher iris curvature suggesting a predominant PB mechanism.[40]

We further categorized the enrolled 405 PACS eyes into different subgroups based on the main angle closure mechanisms. 129 eyes were found to have PB (33.3%), 138 eyes PIC (35.7%), and 120 eyes TPIR (31.0%) as the dominant angle closure mechanism. In addition, five eyes were determined to have an exaggerated lens vault as the dominant angle closure mechanism. The dominant angle closure mechanisms of the rest 13 eyes could not be identified. Considering that the algorithms we describe may have different performances among the three subgroups, we plan to study the accuracy of machine-learning algorithms in different angle closure mechanism subgroups as the next step.

One may argue about the significance of population-based screening of PACS given the low incidence of development of PAC or PACG over 6 years in subjects with PACS found by the Zhongshan Angle Closure Prevention trial.[41] They also suggested that prophylactic LPI on a population basis may not be the best strategy for preventing vision loss in PACS.[41] However, the Zhongshan Angle Closure Prevention trial does not provide sufficient information to estimate the risk in an individual PACS, which is especially important for determining who is at higher risk of a sight-threatening acute attack and should undergo a preventive LPI.[41]

In our opinion, screening for PACS is not useless, but we do need to identify and decide which PACS have a higher risk of developing PAC or vision-threatening acute angle closure. Also, in our study, we were looking for an ideal screening method for PACD, not only for PACS. However, this observational, cross-sectional study was part of a population-based study (the 5-year follow-up of the Handan Eye Study), in which the number of PAC/PACG was limited. We intended to establish and evaluate this new method first in PACS subjects, and in future study, we will further evaluate this screening method in PAC/PACG subjects.

To the best of our knowledge, this is the first study to establish and evaluate novel classification algorithms for detection of PACS by combining multiple static and dynamic anterior segment parameters. The study has several limitations. One is the utilization of semiautomated image analysis software requiring manual localization of the scleral spur that introduces a degree of subjectivity. Another limitation is that we used the two-quadrant definition of PACS and we did not look at other definitions of PACS such as 270° of closure.

Conclusion

In conclusion, we evaluated the ability of a range of static and dynamic ASOCT-derived parameters using three classification algorithms in the screening of PACS. All provided similar results from the same dataset: three models with a set of only four ASOCT parameters showed an AUC of 0.826 to 0.844 for detecting PACS. Although all algorithms failed to reach the requirements for population-based screening, they do provide a promise for basis for future research directed toward the development of an image-based, noncontact method to screen for angle closure.

Acknowledgments

The authors thank Jin Shanshan for her contribution to the statistical design of this study.

Supported by research special fund of the Ministry of Health of the People's Republic of China (grant number 201002019) and National Natural Science Foundation of China (grant number 81900847). The funding organizations had no role in the design or conduct of this research.

Disclosure: **Y. Zhang**, None; **Q. Zhang**, None; **L. Li**, None; **R. Thomas**, None; **S.Z. Li**, None; **M.G. He**, None; **N.L. Wang**, None

References

1. Quigley HA, Broman AT. The number of people with glaucoma worldwide in 2010 and 2020. *Br J Ophthalmol*. 2006;90:262–267.
2. Foster PJ, Johnson GJ. Glaucoma in China: how big is the problem? *Br J Ophthalmol*. 2001;85:1277–1282.
3. Foster PJ, Buhrmann R, Quigley HA, Johnson GJ. The definition and classification of glaucoma in prevalence surveys. *Br J Ophthalmol*. 2002;86:238–242.
4. Thomas R, Parikh R, Muliyil J, Kumar RS. Five-year risk of progression of primary angle closure to primary angle closure glaucoma: a population-based study. *Acta Ophthalmol Scand*. 2003;81:480–485.
5. Thomas R, George R, Parikh R, Muliyil J, Jacob A. Five year risk of progression of primary angle closure suspects to primary angle closure: a

population based study. *Br J Ophthalmol*. 2003;87:450–454.
6. Weinreb RN, Healey PR, Topouzis F. *Glaucoma screening. World Glaucoma Association consensus series 5*. The Hague, Netherlands: Kugler: 2008.
7. Thomas R, Arun T, Muliyil J, George R. Outcome of laser peripheral iridotomy in chronic primary angle closure glaucoma. *Ophthalmic Surg Lasers*. 1999;30:547–553.
8. Nolan WP, Foster PJ, Devereux JG, Uranchimeg D, Johnson GJ, Baasanhu J. YAG laser iridotomy treatment for primary angle closure in East Asian eyes. *Br J Ophthalmol*. 2000;84:1255–1259.
9. Winegarner A, Miki A, Kumoi M, et al. Anterior segment Scheimpflug imaging for detecting primary angle closure disease. *Graefes Arch Clin Exp Ophthalmol*. 2019;257:161–167.
10. Friedman DS, He M. Anterior chamber angle assessment techniques. *Surv Ophthalmol*. 2008;53:250–273.
11. Lavanya R, Foster PJ, Sakata LM, et al. Screening for narrow angles in the Singapore population: evaluation of new noncontact screening methods. *Ophthalmology*. 2008;115:1720–1727.
12. Thomas R, Parikh R, Paul P, Muliyil J. Population-based screening versus case detection. *Indian J Ophthalmol*. 2002;50:233–237.
13. Zhang Y, Li SZ, Li L, Thomas R, Wang NL. The Handan Eye Study: comparison of screening methods for primary angle closure suspects in a rural Chinese population. *Ophthalmic Epidemiol*. 2014;21:268–275.
14. Lowe RF. Aetiology of the anatomical basis for primary angle closure glaucoma: biometrical comparisons between normal eyes and eyes with primary angle-closure glaucoma. *Br J Ophthalmol*. 1970;54:161–169.
15. Nongpiur ME, He M, Amerasinghe N, et al. Lens vault, thickness, and position in Chinese subjects with angle closure. *Ophthalmology*. 2011;118:474–479.
16. Zhang Y, Li SZ, Li L, He MG, Thomas R, Wang NL. Quantitative analysis of iris changes after physiologic and pharmacologic mydriasis in a rural Chinese population. *Invest Ophthalmol Vis Sci*. 2014;55:4405–4412.
17. Zhang Y, Li SZ, Li L, He MG, Thomas R, Wang NL. Quantitative analysis of iris changes following mydriasis in subjects with different mechanisms of angle closure. *Invest Ophthalmol Vis Sci*. 2015;56:563–570.
18. Zhang Y, Li SZ, Li L, He MG, Thomas R, Wang NL. Dynamic iris changes as a risk factor in primary angle closure disease. *Invest Ophthalmol Vis Sci*. 2016;57:218–226.
19. Brown JS, Filtcroft DI, Ying GS, et al. In vivo human choroidal thickness measurements: evidence for diurnal fluctuations. *Invest Ophthalmol Vis Sci*. 2009;50:5–12.
20. Liang YB, Friedman DS, Wong TY, et al. Rationale, design, methodology, and baseline data of a population-based study in rural China: the Handan Eye Study. *Ophthalmic Epidemiol*. 2009;16:115–127.
21. Radhakrishnan S, Rollins AM, Roth JE, et al. Real time optical coherence tomography of the anterior segment at 1310 nm. *Arch Ophthalmol*. 2001;119:1179–1185.
22. Console JW, Sakata LM, Aung T, Friedman DS, He M. Quantitative analysis of anterior segment optical coherence tomography images: the Zhongshan Angle Assessment Program. *Br J Ophthalmol*. 2008;92:1612–1616.
23. Salim S. The role of anterior segment optical coherence tomography in glaucoma. *J Ophthalmol*. 2012;2012:476801.
24. Wang D, Qi M, He M, Wu L, Lin S. Ethnic difference of the anterior chamber area and volume and its association with angle width. *Invest Ophthalmol Vis Sci*. 2012;53:3139–3144.
25. Wang YE, Li Y, Wang D, He M, Lin S. Comparison of factors associated with occludable angle between American Caucasians and ethnic Chinese. *Invest Ophthalmol Vis Sci*. 2013;54:7717–7723.
26. Ozaki M, Nongpiur ME, Aung T, He M, Mizoguchi T. Increased lens vault as a risk factor for angle closure: confirmation in a Japanese population. *Graefes Arch Clin Exp Ophthalmol*. 2012;250:1863–1868.
27. Sun JH, Sung KR, Yun SC, et al. Factors associated with anterior chamber narrowing with age: an optical coherence tomography study. *Invest Ophthalmol Vis Sci*. 2012;53:2607–2610.
28. Hastie T, Tibshirani R, Friedman J. *The Elements of Statistical Learning: Data Mining, Inference, and Prediction*. 2nd ed. New York: Springer; 2009.
29. Bursac Z, Gauss CH, Williams DK, Hosmer DW. Purposeful selection of variables in logistic regression. *Source Code Biol Med*. 2008;3:17.
30. Olivera AR, Roesler V, Iochpe C, et al. Comparison of machine-learning algorithms to build a predictive model for detecting undiagnosed diabetes - ELSA-Brasil: accuracy study. *Sao Paulo Med J*. 2017;135:234–246.
31. Heo J, Yoon JG, Park H, Kim YD, Nam HS, Heo JH. Machine learning–based model for prediction

of outcomes in acute stroke. *Stroke*. 2019;50:1263–1265.
32. Kim SJ, Cho KJ, Oh S. Development of machine learning models for diagnosis of glaucoma. *PLoS One*. 2017;12:e0177726.
33. Rahimy E. Deep learning applications in ophthalmology. *Curr Opin Ophthalmol*. 2018;29:254–260.
34. Nongpiur ME, Haaland BA, Friedman DS, et al. Classification algorithms based on anterior segment optical coherence tomography measurements for detection of angle closure. *Ophthalmology*. 2013;120:48–54.
35. Bossuyt P, Davenport C, Deeks J, Hyde C, Leeflang M, Scholten R. Chapter 11:Interpreting results and drawing conclusions. In:Deeks JJ, Bossuyt PM, Gatsonis C ed. *Cochrane Handbook for Systematic Reviews of Diagnostic Test Accuracy Version 0.9.* The Cochrane Collaboration; 2013: 1–30. Available from: http://srdta.cochrane.org/.
36. Guzman CP, Gong T, Nongpiur ME, et al. Anterior segment optical coherence tomography parameters in subtypes of primary angle closure. *Invest Ophthalmol Vis Sci*. 2013;54:5281–5286.
37. Lin J, Wang Z, Chung C, Xu J, Dai M, Huang J. Dynamic changes of anterior segment in patients with different stages of primary angle-closure in both eyes and normal subjects. *PLoS One*. 2017;12:e0177769.
38. Baek S, Sung KR, Sun JH, et al. A hierarchical cluster analysis of primary angle closure classification using anterior segment optical coherence tomography parameters. *Invest Ophthalmol Vis Sci*. 2013;54:848–853.
39. Nongpiur ME, Gong T, Lee HK, et al. Subgrouping of primary angle-closure suspects based on anterior segment optical coherence tomography parameters. *Ophthalmology*. 2013;120:2525–2531.
40. Moghimi S, Torkashvand A, Mohammadi M, et al. Classification of primary angle closure spectrum with hierarchical cluster analysis. *PLoS One*.2018;13:e0199157.
41. He M, Jiang Y, Huang S, et al. Laser peripheral iridotomy for the prevention of angle closure: a single-centre, randomised controlled trial. *Lancet*. 2019;393:1609–1618.